The Radiation Fields of Discone Antenna as Feed By Dipole

Ra'ed A. Al-Assdi
Dept. of physics, College of Science, University of Basrah.
raedalassdimar@yahoo.com

Abstract

Computational electromagnetics (CEM) may be broadly defined as the branch of electromagnetics that intrinsically and routinely involves using a digital computer to obtain numerical results. This paper presents a technique for the measurement of the radiation fields of discone antenna by using moment method (MM). The measurements are carried out for the perfect conductors by using the dipole feed. The numerically calculated results are experimentally validated for a discone antenna from 300MHz - 2.4GHz. The radiation patterns of discone antenna for multiple frequency and the effects of feed location on antenna's operations are discussed.

Keyword:- **A**ntenna , **D**iscine antenna , **B**iconical antenna

1- Introduction

With the evolutionary development of (CEM) during the past 40-plus years, the ever-increasing complexity of communication systems, there has been a need for engineers to predict the behavior of such systems by means of computer simulations. As a result, the equations involved in the mathematical description of electromagnetic quantities, which are of interest in most cases, have become more complex. Consequently, more sophisticated numerical methods have been developed to solve electromagnetic problems. These methods are gaining greater and greater success with the constant development of new powerful digital computers[1].

A discone antenna is in fact a biconical antenna where one of the cones is replaced by a disk-shaped ground plane, with impedance and radiation characteristics detrained by the angle of the cone and the diameter of the disc. The length of the cone and the dimensions of the feeding structure limit the antenna's lowest and highest frequencies[2]. The disk is mounted on top of the cone as shown in figure(1). This structure was first developed by Kandoian in 1945. Discones have linearly polarized radiation patterns like a monopole. The radiation pattern is near omnidirectional in the azimuth plane for about one octave and the impedance bandwidth can be up to 10:1 [3].

The length of the cone elements should be a quarter-wavelength of the minimum operating frequency. The diameter of the top of the cone depends on the determined upper frequency limit of the antenna: the smaller the diameter, the higher the frequency. The slant height of the cone is equal to a full free-space quarter-wavelength at the lowest frequency of interest[4].

Discone antennas have been used widely for various applications such as amateur radio and wireless systems. Because of its wideband characteristics it is a suitable choice for ultra wideband (UWB) communication. In UWB communication a pulse transmitting antenna is usually necessary. The effects of angular dispersion of discone antennas are studied. One limiting parameter of discone is the feed point. Since the cone is fed by a dipole. The frequency bandwidth is inversely proportional to the size of truncation. To overcome this problem and increase the bandwidth, the configuration shown in figure(2) is suggested. In this design a discone antenna is designed for a higher frequency band of (2.4–9 GHz) and placed upside down with a shared feeding point with the larger discone. The larger discone is designed for a lower frequency band of 300 MHz to 2.4 GHz [3].

In this work moment method (MM) technique is used to compute the radiation field from asymmetrically excited perfectly conducting bodies of revolution with different frequency and feed locations[5].

2- Formulation:

The problem of electromagnetic radiation and scattering from perfectly conducting bodies of revolution of arbitrary shape is considered. The mathematical formulation is an integro-differential equation, obtained from the potential integrals plus boundary condition at the body[6].

The numerical methods has been developed to treat the electromagnetic of scattering and radiation problems from surfaces. When a scattering surface supports the nonvanishing electric current $\bar{J}$ and the magnetic current $\overline{M}$, the scattered electric field may be obtained from [6], with a suppressed time variation of ($e^{j\omega t}$) as:

$$\overline{E}^{s}(\bar{r}) = -j\omega\overline{A}(\bar{r}) - \nabla V - \nabla X\overline{F}$$
……..(1)

Where $\overline{A}$ and $\overline{F}$ are the magnetic and the electric vector potentials, and V is the electric scalar potential. The functions of the coordinate on the scatterer can be written as[7]:

$$\hat{n}\times\overline{E}^{inc} = -\hat{n}\times\left[j\omega\mu\int_s \bar{J}\Phi ds' - \frac{\nabla}{j\omega\varepsilon}\int_s (\nabla'_s\cdot\bar{J})\Phi ds' - \nabla x\int_s \overline{M}\Phi ds' \right] \quad \text{……..(2)}$$

Where $\bar{J}$ and $\overline{M}$ are the electric and magnetic surface current, Φ is the free-space Green's function. When a field point approaches the scattering surface from the inside, the boundary condition $\overline{E}=0$ is satisfied. For bodies of revolution BoR both the incident field $\overline{E}^{inc}$ and the induced current $\bar{J}$ can be expressed due to Fourier series of the azimuthal coordinate. This approach provides an integral equation for each azimuthal mode, the solution of which gives the unknown mode current. This method is especially suited to conical horn antennas, since they normally operate in the dominant mode. On a body of revolution the induced current $\bar{J}$ has components along two orthogonal surface vectors $\hat{t}$ and $\hat{\phi}$. According to the moment method each component can be represented by a finite set of expansion functions. Mautz an Harrington [6] have selected these expansion functions ($\bar{J}^{t,\phi}_{nj} = \hat{U}_{t,\phi} f_j(t) e^{jn\phi}$), by using the set testing functions ($\overline{W}^{t,\phi}_{ni} = \hat{U}_{t,\phi} f_i(t) e^{-jn\phi}$) produced from Galerkin expansions. Utilizing a similar procedure, one can reduce eq.(2) to matrices form[7]:

$$\begin{bmatrix} \left[Z^{tt,J}_m\right]+\left[Z^{tt,M}_m\right] & \left[Z^{t\phi,J}_m\right]+\left[Z^{t\phi,M}_m\right] \\ \left[Z^{\phi t,J}_m\right]+\left[Z^{\phi t,M}_m\right] & \left[Z^{\phi\phi,J}_m\right]+\left[Z^{\phi\phi,M}_m\right] \end{bmatrix} \begin{bmatrix} \left[I^t_m\right] \\ \left[I^\phi_m\right] \end{bmatrix} = \begin{bmatrix} \left[V^t_m\right] \\ \left[V^\phi_m\right] \end{bmatrix}$$
……..(3)

Where the superscripts J and M refer to the submatrices of the electric and magnetic currents respectively. In the above equation the submatrices $\left[Z_m^{tt}\right]$, $\left[Z_m^{t\phi}\right]$, $\left[Z_m^{\phi t}\right]$ and $\left[Z_m^{\phi\phi}\right]$ are known as the impedance matrix of the mode *m*, $\left[I_m^t\right]$ and $\left[I_m^\phi\right]$ are column matrices of the unknown coefficients in the expansion of the current and $\left[V_m^t\right]$ and $\left[V_m^\phi\right]$ are excitation matrices which can be evaluated as [5]:

$$\left(Z_m^{\alpha\beta}\right)_{ij} = \left\langle \overline{W}_{mi}^{\alpha}, L(J_{mj}^{\beta})\right\rangle$$

……..(4)

$$\left(V_m^{\alpha}\right)_i = \left\langle \overline{W}_{mi}^{\alpha}, E^{inc}\right\rangle$$

……..(5)

Where α and β denoted t or ϕ. We assume that the field incident on the body of revolution is due to an x-directed electric dipole of moment $\bar{I}dl$ at a point $d(0,0,z_d)$.

Eq.(5) can be written as:

$$\left(V_m^t\right)_i = \left(\frac{-j\eta Idl}{4}\right)\sum_{p=1}^{4}\left[\frac{e^{-jkR_d}}{kR_d}\right]_{i'}\left\{T_p' k\sin\gamma_{i'}\right\} + \left[\frac{\rho_i'}{R_d}\left(\frac{1}{R_d}+jk\right)\right]_{i'} T_{p'}'$$

……..(6)

$$\left(V_m^\phi\right)_i = \pm\left(\frac{\eta Idl}{4}\right)\sum_{p=1}^{4}\frac{1}{k}\left[\frac{e^{jkR_d}}{kR_d}\right]_{i'}\cdot\left[-k^2+\left(\frac{1}{R_d}+jk\right)\frac{1}{R_d}\right]_{i'} T_p'$$

……..(7)

Where $R_d = \left[\rho_{i'}^2 + \left(z_{i'} - z_d\right)^2\right]^{1/2}$ and the mode $m = \pm 1$, (T and T') are the weighting factors of the impulse functions approximating the triangular functions and their derivatives and γ is the angle of the generating curve with the z-axis.

For a body of revolution with impedance boundary conditions the far scattered field in the (θ,ϕ) direction my be written in the form[7]:

$$E_{\theta}^{s}=\frac{-j\omega\mu}{4\pi r}\left[\sum_{m=-M}^{M}\sum_{j=1}^{N}\left[\left(R_{m}^{t\theta}\right)_{j}I_{mj}^{t}+\left(R_{m}^{\phi\theta}\right)_{j}I_{mj}^{\phi}\right]\right]e^{-jkr}$$
……..(8)

$$E_{\phi}^{s}=\frac{-j\omega\mu}{4\pi r}\left[\sum_{m=-M}^{M}\sum_{j=1}^{N}\left[\left(R_{m}^{t\phi}\right)_{j}I_{mj}^{t}+\left(R_{m}^{\phi\phi}\right)_{j}I_{mj}^{\phi}\right]\right]e^{-jkr}$$
……..(9)

Where:

$$\left(R_{m}^{t\theta}\right)_{i}=\sum_{q=1}^{4}C(m,q')\left[j\left(J_{(m+1)}-J_{(m-1)}\right)\sin\gamma_{i'}\cos\theta-2J_{m}\cos\gamma_{i'}\sin\theta\right]$$
……..(10)

$$\left(R_{m}^{\phi\theta}\right)_{i}=-\sum_{q=1}^{4}C(m,q')\left[\left(J_{(m+1)}+J_{(m-1)}\right)\cos\theta\right]$$
……..(11)

$$\left(R_{m}^{t\phi}\right)_{i}=\sum_{q=1}^{4}C(m,q')\left[\left(J_{(m+1)}+J_{(m-1)}\right)\sin\gamma_{i'}\right]$$
……..(12)

$$\left(R_{m}^{\phi\phi}\right)_{i}=\sum_{q=1}^{4}C(m,q')\left[j\left(J_{(m+1)}-J_{(m-1)}\right)\right]$$
……..(13)

With $J_{m}=J_{m}(k\rho_{i'}\sin\theta)$ is Bessel function of order m , and :

$C(m,q')=\pi j^{m}e^{jm\phi}e^{jkz_{i'}\cos\theta}T_{q'}$

$q'=q+4i-4$

$i'=q+2i-2$

The sequence of equations completes the derivation of the scattered field for a body of revolution with impedance boundary conditions[7].

To prove the mathematical and practical treatment correctness which has been taken into account in this paper. Consider the discone antenna which is a special case of biconical antennas, whose radiation characteristics are mainly detrained by the angle of the cone and the diameter of the disc. Therefore, the radiation pattern for spherically capped biconical antenna with unequal cone angles($\psi_{1}=53.1^{\circ}$ and $\psi_{2}=90^{\circ}$), was shown in Figure (3-a)[8][9]. Another good correctness was examine by choosing the dimensions of a discone taken by [3][10], but with dipole feed, as shown in figure (3-b)

3- Numerical Results:

Impedance and radiation of a symmetrical discone antenna (as shown in figure(2) can be calculated using moment method formula with Galerkin technique. The discone antenna is an excellent theoretical model for studying the essential by using property of a dipole-type antenna. The optimum dimensions of the antenna under test were choosing with length of 0.23 cm, cone angle (α) of 30◦, ground plane diameter of 0.29 cm and the distance between the cone and ground plane is 0.025 cm.

The discone antenna here is designed for a lower frequency band of 300 MHz to 2.4 GHz. Using the computer simulation, the radiation patterns of the optimized antenna for multi frequency with a dipole location of 0.0255 cm from the center of axis are shown in figure (4).

The results show that the perfect case was obtained at a frequency of 500 MHz in this design. Therefore, this frequency was chosen to study the influence of the dipole locations on the radiation fields of the discone antenna as shown in figure (5).

4- Conclusions:

The solution of large and small scale electromagnetic (EM) integral equation problems by the moment method is burdened by the creation and storage of a dense system impedance matrix. This paper presents a new case for efficiently compressing the result of the discone antenna by using dipole feed. The operator equation is solved by the moment method. The solution , valid for three- dimensional closed surface ***S***, is then applied to a surface of the BoR.

It is found that the microwave measurement done at a multi frequency generates a number of solutions for the location of dipole. Hence measurements must be carried out at more than one frequency and location of dipole to get the correct answer for the radiation.

4- References:

[1] Michel M. Ney, "***Method of Moments as Applied to Electromagnetic Problems*** " , IEEE Trans. Anten. and Propag., Vol. MTT-33, No. 10, pp. 972-980, 1985.

[2] Xianming Qing, Zhi Ning Chen and Michael Yan Wah Chia, " ***UWB Characteristics of Disc Cone Antenna*** ", IEEE International Workshop on Antenna Technology, pp. 97-100, 2005.

[3] Constantine A. Balanis, "***Modern Antenna Handbook***", John Wiley & Sons, Inc., New York, 2008.

[4] John L. Volakis and Thomas F. Eibert , "***Antenna Engineering Handbook***", McGraw-Hill Companies, New York, 2007.

[5] Medgysi-Mitschang, L. N. and Wang, D., " ***Radiation and Scattering from Asymmetrically Excited Bodies of Revolution*** ", IEEE Trans. Anten. and Propag. pp. 90-93, 1976.

[6] Mautz, J. R. and Harrington, R. F., " ***Radiation and Scattering from Bodies of Revolution*** " , Appl. Sci. Res., Vol. 20, pp. 405-435, 1969.

[7] Kamal A. Iskander, Lotfollah Shafai, Aksel Frandsen and Jesper E. Hansen, " ***Application of Impedance Boundary Condition to Numerical Solution of Corrugated Circular Horns***" , IEEE Trans. Anten. and Propag., Vol. AP-30, No. 3, pp. 366-372, 1982.

[8] Surendra N. Samaddar and Eric L. Mokole, "***Biconical Antenna with Unequal Cone Angles*** " , IEEE Trans. Anten. and Propag., Vol. 46, No. 2, pp. 181-193, 1998.

[9] Debalina Ghosh, Tapan K. Sarkar and Eric L. Mokole, "***A Spherically-Capped Discone Antenna for Ultra-Wideband Operation*** " , www.pdfgeni.com/book/discone-antenna-pdf.html.

[10] Jiun Kim and Seon-Ook Park, "***Novel Ultra-Wideband Discone Antenna*** " , Microwave and Optical Technology Letters, Vol. 42, No. 2, pp. 113-115, 2004.

المستخلص

الحسابات الكهرومغناطيسية يمكن أن تعرف بوضوح على إنها فرع من الكهرومغناطيسية التي تشمل استخدام الحاسبات الرقمية بشكل جوهري وروتيني للحصول على النتائج العددية. هذا البحث يقدم تقنية لحساب مجالات الإشعاع الصادرة من هوائي قمعي-عاكس وذلك باستخدام طريقة العزوم. علما القياسات التي اعتمدت قد اختيرت للأجسام ذات التوصيل الجيد وذلك بعد استخدام ثنائي القطب كمغذي للهوائي. إن نتائج الحسابات العددية لهوائي قمعي-عاكس اعتمدت تجريبيا على استخدام الترددات ضمن 300MHz - 2.4GHz. تم مناقشة الحسابات والنتائج

لهوائي قمعي-عاكس من خلال هيكل الإشعاع عند تغير التردد وكذلك اختيار مواقع مختلفة للمغذي وتأثيرها على عمل الهوائيات.

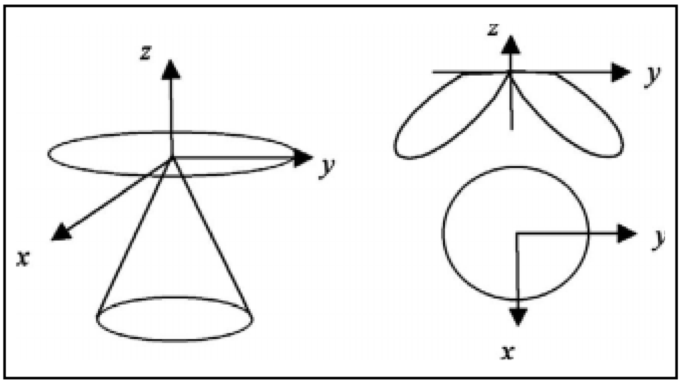

Figure (1) Typical radiation patterns of discone antenna[3].

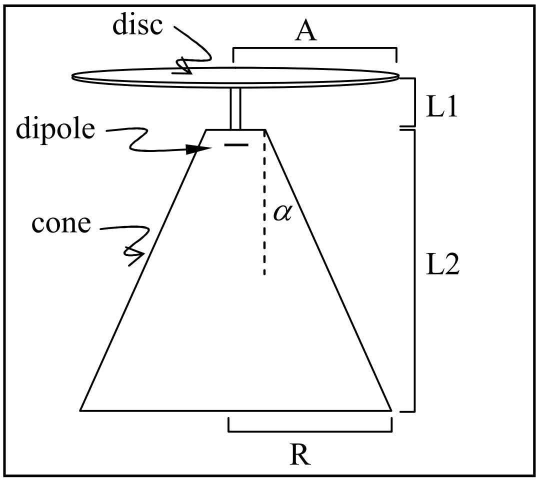

Figure (2) Design and optimization of the discone antenna

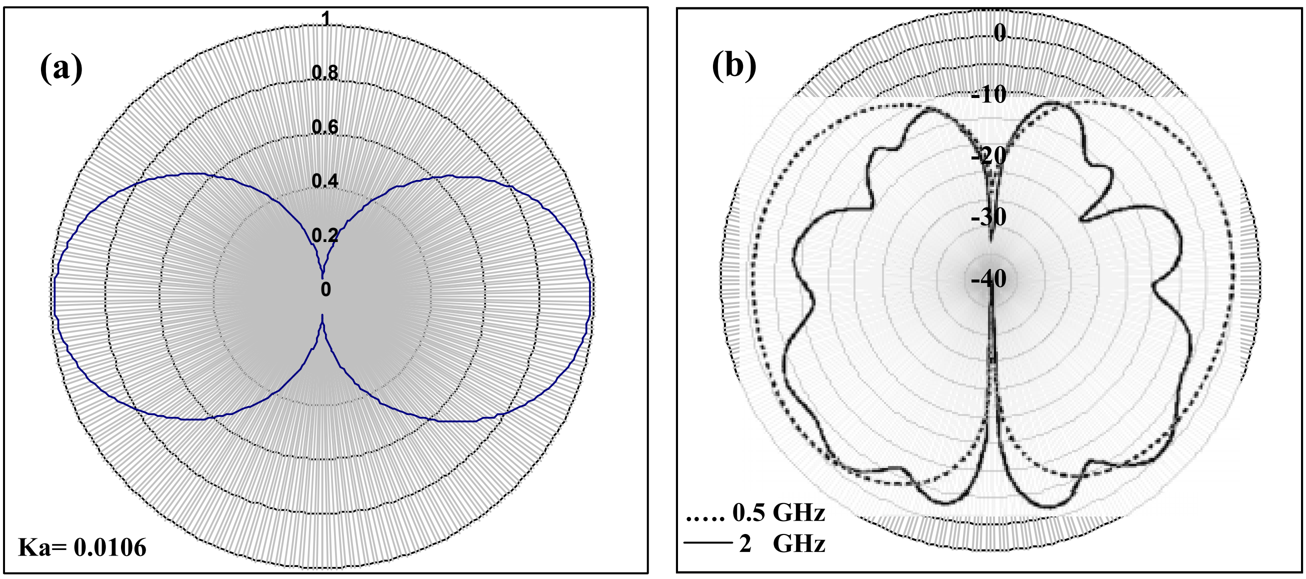

Figure (3) Elevation radiation patterns of:
(a) spherically capped biconical antenna with unequal cone angles[8][9]
(

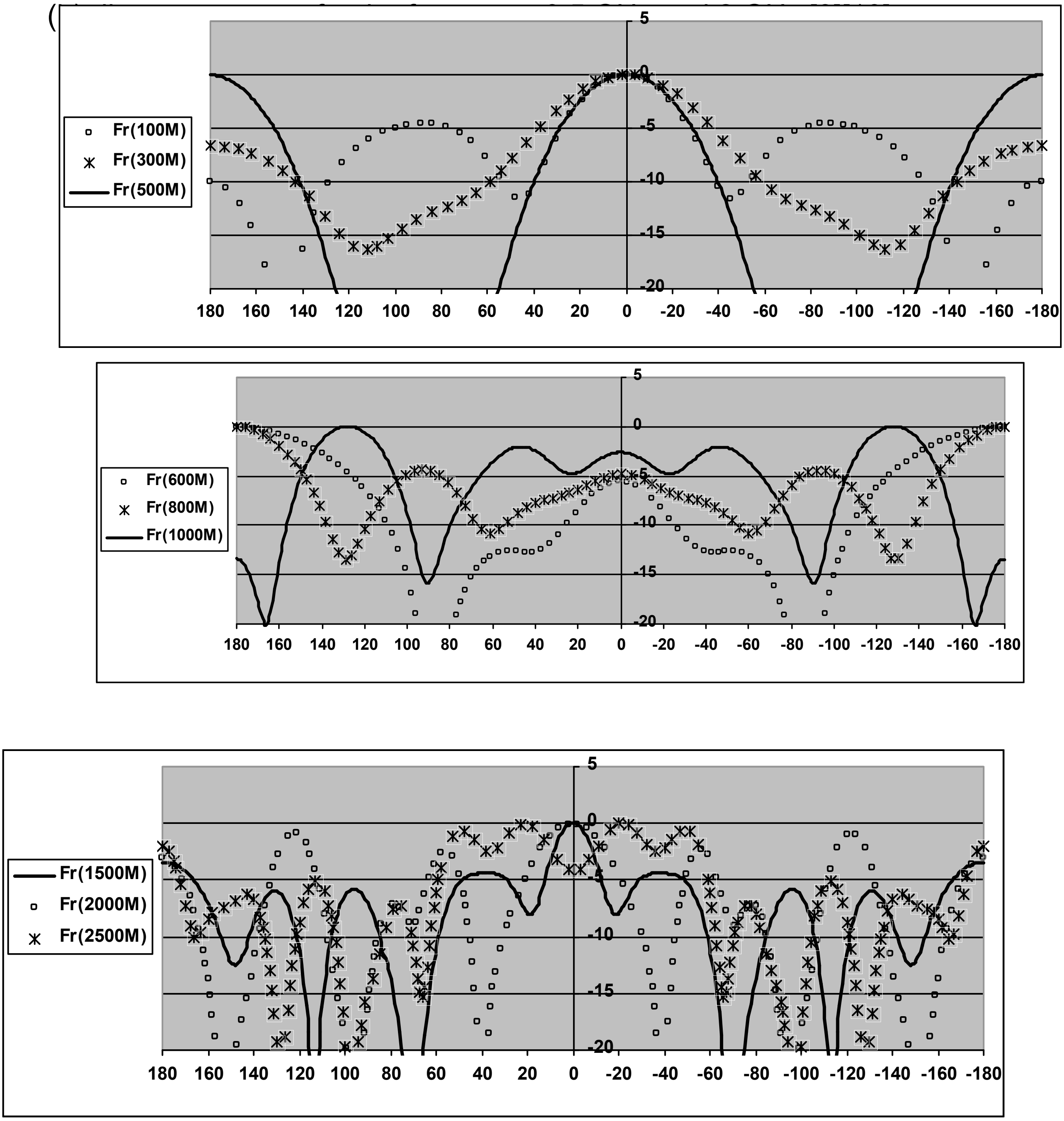

Figure (4) Elevation radiation patterns of discone antenna for multi frequency

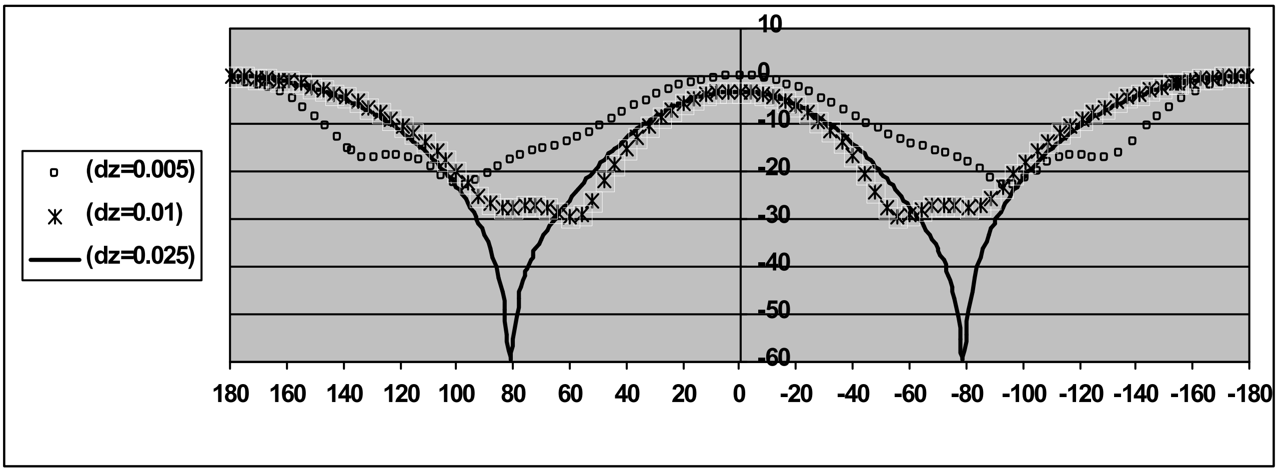

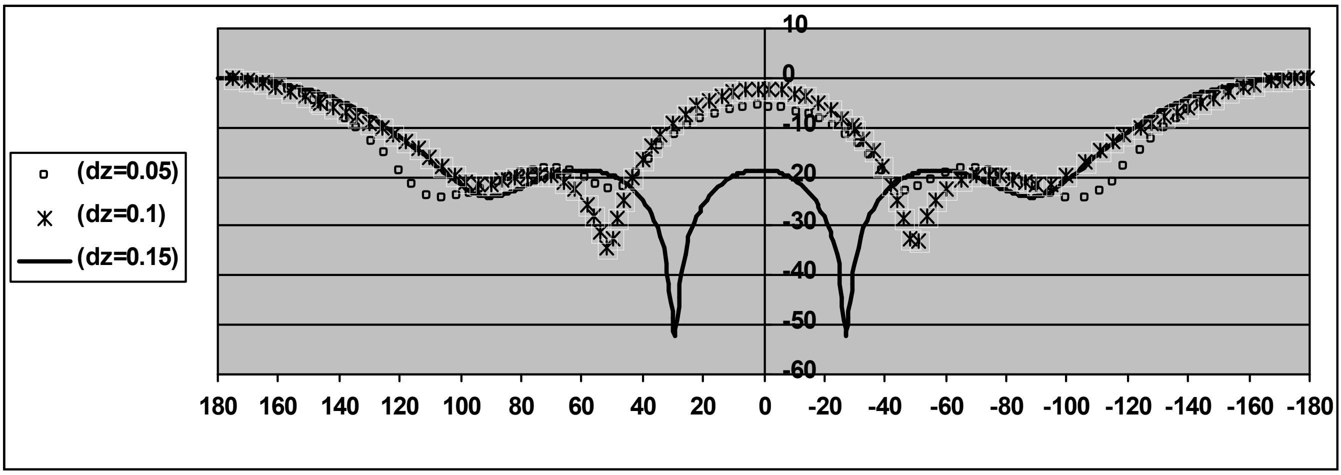

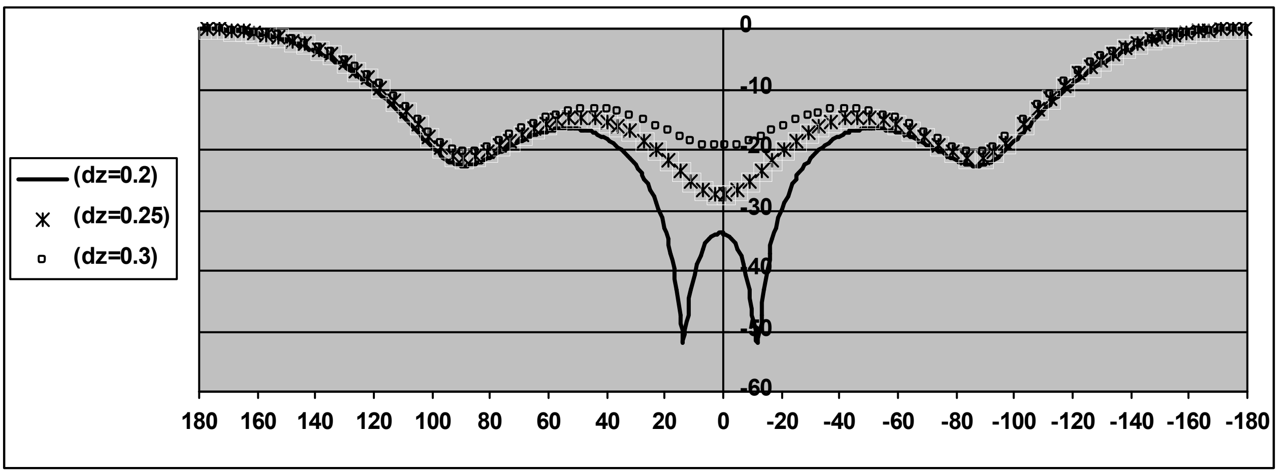

Figure (5) Elevation radiation patterns of discone antenna for deferent of the dipole locations